SPECIAL FEATURE: PERSPECTIVE

Archaeological climate proxies and the complexities of reconstructing Holocene El Niño in coastal Peru

Daniel H. Sandweiss[a,b,1], C. Fred T. Andrus[c], Alice R. Kelley[b,d], Kirk A. Maasch[b,d], Elizabeth J. Reitz[e], and Paul B. Roscoe[a,b]

Edited by Dolores R. Piperno, Smithsonian Institution, Washington, DC, and approved November 22, 2019 (received for review August 14, 2019)

Archaeological evidence plays a key role in longitudinal studies of humans and climate. Climate proxy data from Peruvian archaeological sites provide a case study through insight into the history of the "flavors" or varieties of El Niño (EN) events after ∼11 ka: eastern Pacific EN, La Niña, coastal EN (COA), and central Pacific or Modoki EN (CP). Archaeological proxies are important to the coastal Peruvian case because more commonly used paleoclimate proxies are unavailable or equivocal. Previously, multiproxy evidence from the Peruvian coast and elsewhere suggested that EN frequency varied over the Holocene: 1) present in the Early Holocene; 2) absent or very low frequency during the Middle Holocene (∼9 to 6 ka); 3) low after ∼6 ka; and 4) rapidly increasing frequency after 3 ka. Despite skepticism about the reliability of archaeological proxies, nonarchaeological proxies seemed to confirm this archaeological EN reconstruction. Although there is consensus that EN frequency varied over this period, some nonarchaeological and archaeological proxies call parts of this reconstruction into question. Here we review Holocene EN frequency reconstructions for the Peruvian coast, point to complexities introduced by apparent contradictions in a range of proxy records, consider the impact of CP and COA phenomena, and assess the merits of archaeological proxies in EN reconstructions. Reconciling Peruvian coastal paleoclimate data is critical for testing models of future EN behavior under climate variability.

climate proxies | archaeology | El Niño | Peru | Holocene

The large-magnitude, canonical, eastern Pacific (EP) El Niño (EN) events of 1982 to 1983 and 1997 to 1998 captured global attention and injected EN into popular culture (e.g., ref. 1). Although some climate modelers, paleoclimatologists, biologists, geographers, archaeologists, and other scientists were interested in EN earlier in the 20th century, subsequent decades saw an explosion in EN research, coinciding with growing awareness of the impact of anthropogenic climate change and concern over the role of EN/Southern Oscillation (ENSO) in present and future interannual climate variability (e.g., ref. 2). Predicting ENSO behavior under future climate states is a modeling exercise, but as Lu et al. (3) note, paleorecords are both essential and iterative for testing models. As they point out, "South America coastal regions and nearby islands in the tropical eastern Pacific, located in the ENSO center of action, are ideal regions to search for information on past ENSO variability" (ref. 3, p. 3).

Archaeological climate proxies are globally useful in multiproxy approaches to reliable reconstruction of past climates (4). Hambrecht et al. (5) dub archaeological sites "distributed long-term observing networks of the past." In places like the Peruvian coast, where nonanthropogenic proxies are absent, scarce, incomplete, or compromised (6), archaeological climate proxies are essential. Indeed, the earliest indication of EN Holocene variability came from archaeologically recovered marine fauna from the north coast of Peru (7, 8). Later, a meta-analysis of mollusk remains from Peruvian coastal sites furnished early evidence for an increase in EP frequency at about 3.0 ka (9). A Google Scholar search on 3.0 ka and EN yields multiple studies identifying

[a]Department of Anthropology, University of Maine, Orono, ME 04469; [b]Climate Change Institute, University of Maine, Orono, ME 04469; [c]Department of Geological Sciences, University of Alabama, Tuscaloosa, AL 35487; [d]School of Earth and Climate Sciences, University of Maine, Orono, ME 04469; and [e]Georgia Museum of Natural History, University of Georgia, Athens, GA 30602

Author contributions: D.H.S., C.F.T.A., K.A.M., and E.J.R. designed research; D.H.S., C.F.T.A., A.R.K., K.A.M., and E.J.R. performed research; D.H.S., C.F.T.A., A.R.K., K.A.M., E.J.R., and P.B.R. analyzed data; and D.H.S., C.F.T.A., A.R.K., K.A.M., E.J.R., and P.B.R. wrote the paper.

The authors declare no competing interest.

This article is a PNAS Direct Submission.

Published under the PNAS license.

[1]To whom correspondence may be addressed. Email: dan.sandweiss@maine.edu.

This article contains supporting information online at https://www.pnas.org/lookup/suppl/doi:10.1073/pnas.1912242117/-/DCSupplemental.

Downloaded by guest on April 13, 2020

Fig. 1. Map showing locations mentioned in the text.

coherent change at this time. In 2004, archaeological fish assemblages from Lo Demás (Fig. 1) identified a slight EP frequency increase at 1500 CE (10), later confirmed by marine sediments from an ocean core near the Galápagos (11).

In addition to contributing paleoclimate records, archaeological climate proxies are directly associated with past human behavior, so they can help explain past human ecodynamics (e.g., ref. 12, p. 1085–1086) and adaptations to climate variability and threats. Such studies indicate, for instance, that migration was a common climate-change response in the past, rendering present-day immigration policies dubious if they are based only on suppositions about the permanency of state autonomy and citizenship (13). Other surveys find that leadership and institutional quality (e.g., levels of corruption, political competence, and political turmoil) were critical in the ability of human systems to respond to climate and other environmental perturbations, especially for groups dependent on irrigation systems supporting monocrop subsistence and demanding high levels of management, hierarchy, capital, or labor to maintain and rebuild (14). Archaeological studies indicate that the fiscal foundations of governance and power are critical for successful recovery. Centralized political systems relying on funds from internal resources (e.g., broad-based taxation or corvée labor) are more resilient to climate and other environmental and social perturbations than those in which rulers draw from external resources like trade routes, payments from allies, war booty, private or slave estates, and spot resources (15). Accurate reconstructions of past climate, environment, and human–environment interaction are fundamental to understanding these and related social processes.

ENSO Flavors, Expression on the Peruvian Coast, and Human Impact

For millennia, 2 complementary resource bases have sustained large and complex human populations along the Peruvian coastal desert: fishing in the rich waters of the Peru Current and irrigation-based farming in transecting river valleys. The coast exhibits a significant climate divide at about 12°S (e.g., refs. 16–20), with coastal oceanographic and climate changes more pronounced to the north. During normal (non-EN) years, the Peru Current flows north along the Chilean and Peruvian coasts, bringing cool, deep, nutrient-rich water to the surface through intense upwelling; under these conditions, the thermocline is near the surface. This nutrient upwelling drives the rich Peruvian fishery, while the cool water plus the rain shadow of the Andes creates the stark coastal desert. These normal states are interrupted with varying frequency and intensity by EN, with potential for significant impact on both marine and terrestrial resources.

Climatologists identify multiple components of ENSO, including at least 4 "flavors" of EN: eastern Pacific EN (EP), coastal EN (COA), central Pacific or Modoki EN (CP), and La Niña (LN).

EP. EP events are characterized by weakened trade winds and anomalous warming in the central Pacific that propagates eastward to the Americas. During EP events a warm-water pulse reaches the Peruvian coastal zone, the thermocline deepens, and upwelling weakens. As a result, sea surface temperature (SST) warms, nutrients diminish, and marine biomass decreases throughout the food chain (e.g., refs. 21 and 22). This reduces resources for all organisms, including humans. Increases in SST and rainfall during EP EN have a marked latitudinal gradient and are generally strongest to the north and weaker to the south. Particularly, north of 12°S fisheries may collapse, whereas south of 12°S artisanal fishers may sustain their fishery with replacement species, as they did at Cerro Azul during and after the EP in 1982 to 1983 (23).

Around the Pacific basin, normal precipitation patterns tend to reverse in an EP event: The western Pacific becomes drier, while the eastern Pacific, including the Peruvian coast, becomes wetter. The decline in marine productivity, particularly north of 12°S, is accompanied by terrestrial destruction. Warmer coastal waters support convective storms onshore leading to destructive flooding across the normally arid landscape with consequent damage to coastal infrastructure such as irrigation and field systems. Floods transport massive quantities of sediment into coastal rivers and down to the sea, forming temporary deltas along the shore. Some delta sediments are subsequently carried north by wind and currents to form beach ridges parallel to the shore (24–26). Wells used archaeological settlement patterns to demonstrate how flooding of the Santa River created new land at the river's delta, which people subsequently settled (27). A similar process occurred on the Chira Beach ridge plain (28, 29). Standing water from torrential rainfall and flooding has its own hazards, destroying crops and promoting insect-borne diseases (e.g., refs. 30 and 31).

COA. In February and March of 2017, the coast of Peru was devastated by an event that looked—from local perspectives—like a large-magnitude EP event but that climatologically was quite different. During this COA, the coast experienced extraordinarily high SSTs and torrential rainfall, especially north of 12°S (*SI Appendix*, Figs. S1–S3 show COA SST anomalies to be strongest at and north of 12°S). Central Pacific SSTs, however, remained normal. Reanalysis of records from 1979 to 2017 revealed 7 COAs, some of which followed large-magnitude EP events and prolonged the

Downloaded by guest on April 13, 2020

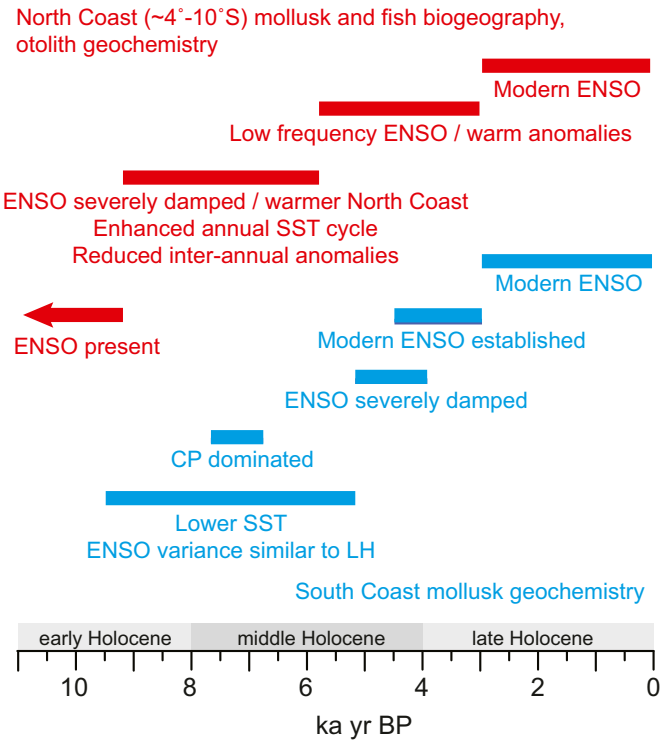

Fig. 2. EP/COA frequency reconstruction from archaeological climate proxies for the Peruvian north coast (red) (6–10) and south coast (blue) (61).

negative consequences for coast dwellers (32). The large-magnitude 1925 EN was also a COA (33), suggesting that COAs may not be related to global warming. At the end of the 2017 COA event, the Peruvian government reported "158 flood-related deaths, 1,372,260 people displaced, and 3.124 billion dollars in damage" (34, 35)—over 1% of Peru's gross domestic product.

From the perspective of Peruvian coast dwellers, especially those north of 12°S, COA and EP events are indistinguishable: Fishing is diminished, coastal infrastructure is damaged or destroyed, insect-borne diseases are rampant, and sediment transport drives coastal progradation. The fact that COA SST anomalies are confined largely to the coast north of 12°S may account for the significant climate divide at that point. Soil development (20), *lomas* plant communities (17, 18), and records of marine productivity and SST in cores from the continental shelf (e.g., refs. 16 and 19 and Fig. 2) all differ north and south of 12°S.

CP. In the early 2000s, Japanese scientists recognized another flavor of ENSO: CP, or Modoki EN (36, 37). During a CP event, the central Pacific warms anomalously, but the warm water does not propagate to the Peruvian coast; Peru does not experience positive SST anomalies during CP EN. CP events do have atmospheric teleconnections around the Pacific Basin, however, which decrease precipitation in the Andes highlands, generally producing drier conditions (e.g., refs. 36–40) and significant reductions in stream flow to the coast (41, 42). Because CP events negatively affect irrigation-based agriculture on the north coast today, they likely would have done so if they occurred in the past.

LN. LN is the reverse of EP: an exaggeration of normal (non-EN) conditions (43, 44). Instead of anomalous warming, the Pacific Basin cools and the EP margin (including Peru) becomes drier (2). On the Peruvian coast, the human consequences of LN are much less severe than EP. Malarial epidemics are not reported for LN (30), but health consequences on the north coast include respiratory problems (45). Fisheries are enhanced by the intensified LN cooling, although agricultural outcomes are mixed (45).

Paleoclimate Proxies and EP/COA in Coastal Peru

Robust paleoclimate data are essential to understanding Earth system history, modeling future climate states, and learning how past societies responded to climate change. To detect paleoclimate events prior to the instrumental record, climate scientists use proxy data from natural archives. These proxies do not measure earlier climate conditions directly, but they contain biological, geological, and historic records of former climates that can be determined through chemical and physical analyses.

Paleoclimate proxies are found in diverse environments worldwide (*SI Appendix*, Table S1). Lacustrine and marine sediments, peat, ice cores, and archaeological sites may contain several different proxies in one sample. Time intervals captured by these proxies vary widely, from monthly to annual, decadal, or centennial; some may represent only a single episodic event. All proxies require direct dating or dating of closely associated materials to provide a time frame for the associated paleoclimate information. Well-dated climate proxies provide a robust record of local to regional climate change.

The desert coast of Peru lacks many common paleoclimate proxies, making it difficult to track EP/COA frequency and magnitude through the Late Pleistocene and Holocene. The normally low SST of the Peru Current precludes coral growth, for example, while limited rainfall hinders widespread accumulation of organics. Standing water bodies, such as marshes and bogs, are rare and mostly ephemeral, capture only large, extremely local precipitation, or were formed by irrigation canals that add an anthropogenic component to their signals. Speleothems that might provide detailed hydrologic information are limited to carbonate terrains, which are rare along the Peruvian coast, while any that exist at high elevations may mix both Atlantic and Pacific signals.

Coastal marine sediment cores largely record changes in river discharge, but temporal resolution is variable because sediment packages represent intervals of uneven time spans. Terrestrial inputs can include both seasonal and EN components, making intense, though normal, summer melt difficult to differentiate from small-scale EN events. These records are thus hard to associate with specific coastal locations and EN events, as even the same flavor of EN affects sectors of the coast differentially across space and time. Use of marine cores in Peruvian Holocene climate reconstruction is limited because all of those north of 12°S and all but one (46) of those south of 12°S show a Middle Holocene hiatus resulting from very low or anomalous sedimentation (e.g., refs. 16, 19, and 47–50).

Fluvial stratigraphic sequences are found in coastal arroyos, but these contain little organic material and the sediments are frequently reworked. In stratified archaeological sequences, the origins of most organics are uncertain, making it difficult to date depositional sequences (e.g., note reversals in table 2 of ref. 51, but see ref. 52). Limited exposure to sunlight during rapid EN flood deposition complicates optically stimulated luminescence (OSL) dating in these settings, although Huckleberry et al. (53) successfully used OSL and infrared stimulated luminescence to date sediments in northern Peruvian canals to late pre-Hispanic and colonial times.

Downloaded by guest on April 13, 2020

Proxy records of EN variability have been developed from highland lake sediments near the equator in the southern Ecuadorian Andes (54–56) and from tropical Andean ice cores (57, 58), but Atlantic/Pacific weather pattern complexity adds uncertainty to reconstructions of EN frequency and variability in general and Middle Holocene EP (and COA) in particular. Lake Pallcacocha is east of the continental divide and influenced by both Atlantic and Pacific air masses. Using a Lake Pallcacocha sediment core, Rodbell et al. (54) proposed that increased precipitation during EP events produced clastic flood layers. They (54) and Moy et al. (55) used clastic layers in the same lake to estimate EN frequencies over the last 11.5 ka, finding them less frequent in the Early Holocene and more frequent after around 5 ka. Due to the complex pattern of Andean precipitation and significant influences from both Atlantic and Pacific water vapor sources, however, interpreting these layers as the direct result of EP is questionable. To investigate further, Schneider et al. (56) produced an independent flood record from Lake Pallcacocha along with a new flood record from adjacent Lake Fondococha. They agreed with Rodbell et al. (54) that the layers resulted from hyperpycnal flows following heavy rains but concluded that precipitation thresholds for moving the sediment remain unknown. In addition, the relationship between intense rain events and EN is unclear: Schneider et al. (56) found that daily precipitation data from nearby meteorological stations suggest these events tend to occur with equal probability during EN warm and cold phases and during neutral EN conditions.

Another unresolved problem with interpreting lake cores is the importance of large-scale (synoptic) vs. regional (mesoscale) controls on extreme precipitation events and their frequency during not only EP and LN but also other flavors of EN. Kiefer and Karamperidou (59) used the Weather and Research Forecasting model (WRF) to dynamically downscale a global reanalysis of atmospheric circulation and precipitation response for each EN flavor. Using WRF to simulate EN events during peak EP, COA, CP, and LN phases, they found precipitation response to EN is type-specific. During EP and COA events warm SSTs lead to intense convective storms on the western Andean slopes. For CP and LN events, though, increased large-scale stratiform precipitation related to mesoscale convective systems (MCS) in the Amazon Basin falls on the eastern Andean slopes. Embedded convective cells within MCS can also produce heavy precipitation. These results complicate the interpretation of paleo-EN proxies from equatorial Andean lake records. Untangling the complex sediment-delivery response to these lakes requires multiple proxies from other locations far afield and underscores the importance of developing proxy records for coastal Peru from materials taken directly from the coast.

Andean ice cores are used to construct paleoclimate proxy records of EN based primarily on oxygen isotope values ($\delta^{18}O$). The highest temporally resolved ice core, from the Quelccaya Ice Cap (QIC) in the Cordillera Vilcanota (5,670 m above sea level), spans the last 1,800 y. Thompson et al. (58) link annually resolved QIC $\delta^{18}O$ to tropical EP SST. Physical mechanisms tying SST to $\delta^{18}O$ in the ice are questioned, however, mainly because of the source and initial isotopic values of water vapor ultimately incorporated into clouds, the amount and seasonality of precipitation falling from the clouds onto the icecap, and the temperature dependence of isotopic fractionation of the water vapor along the path from evaporative source to condensation and snow formation.

A proxy system model to explore how such factors contribute to $\delta^{18}O$ variability in QIC snow suggests that over two-thirds of the $\delta^{18}O$ signal can be attributed to varying strength of upstream convection related to the South American monsoon (60), which brings Atlantic-sourced moisture from the Brazilian highlands into the Andes during the wet season (December through February). The model shows that increased convection over the Amazon during LN increases negative $\delta^{18}O$ in QIC snow, while higher initial isotopic values for EP result in more positive $\delta^{18}O$. Any relationship between EN and QIC $\delta^{18}O$ is therefore not interpretable as a simple response to temperature. In addition, an increase in CP precipitation (59) produces a $\delta^{18}O$ signal indistinguishable from that of LN.

Archaeological Proxies for Coastal Peru for EP (and COA) EN

On the arid north coast, archaeological sites provide the best proxy archives for EN for at least the last 11,000 y. At these sites, people concentrated organic remains representative of past regional conditions in datable stratigraphic contexts. Additionally, canals and other anthropogenic structures contain datable organic materials, time-diagnostic artifacts, or both. These archaeological proxies document shifts in the magnitude, timing, and locations of EN and provide pinning points for broad-scale, regional studies (e.g., refs. 8–10, 61, and 62). The 2 most important archaeological proxies in this region for warm (EP and COA) EN frequency are biogeography (e.g., ref. 62) and the geochemistry of marine mollusk valves (e.g., ref. 61) and fish otoliths (e.g., ref. 63).

Biogeography. To reconstruct former environments, archaeologists use dynamic relationships among humans and their environments, behaviors of biological organisms influencing their geographic distribution, and site formation processes. Biogeographical inferences rely on contemporary observations to infer historical relationships among plants, animals, and environments, on the theory that environmental conditions influencing an organism's distribution today might have governed its distribution in the past. In settings such as coastal Peru, where geochemical and other environmental data are limited, unavailable, or difficult to interpret, this premise provides a way to gauge the relative abundance of warm-water and cool-water organisms in zooarchaeological assemblages. If organisms present in an archaeological assemblage are absent from the local biological community today, one possible explanation is environmental change.

This reasoning is strengthened if temporal changes are observed in indicator groups instead of individual species, particularly if additional proxies support the inference at several sites within a region and/or among regions over time. Kenward and Hall (ref. 64, p. 665) define an indicator group as "a natural grouping of organisms selected because it includes a range of stenotopic species which together encompass a wide spectrum of ecological conditions or human activities relevant to the aims of the study being carried out." When indicator groups are used to hypothesize a "mutual climatic range," defined by overlapping habitat preferences shared among members of several indicator groups, this approach becomes yet more reliable.

Sitio Siches (PV 7–19), located at 4°25′S in a biogeographic transition zone between the Panamanian and Peru–Chilean provinces, is a stratified site with an occupational sequence divided into three cultural phases: Amotape (~10.7 to 10.1 ka), Siches (~7.9 to 6.8 ka), and Honda (~5.8 to 5.2 ka) (65). Biogeographic transition zones are frontiers between biogeographic provinces

Downloaded by guest on April 13, 2020

and are characterized by gradients in environmental parameters such as temperature, dissolved oxygen, salinity, turbidity, and productivity (e.g., ref. 66). In this case, the zone forms where the cold, north-flowing Peru Current meets south-flowing, equatorial waters, deflecting the Peru Current westward, away from the South American continent. (Although technically classed as "warm-temperate," the waters of the Peru–Chilean province are cold in comparison to the warmer waters of the Panamanian province, so we refer to the former as cool-water and the latter as warm-water.) As with most biogeographical boundaries, this one is permeable and animals typical of one province can be found in others, though usually in lower numbers or only periodically (67).

Mollusks document several changes over time at Sitio Siches. Within ~30 km of Siches, Terminal Pleistocene deposits associated with Amotape-phase lithics (68, 69) contain 2 estuarine mollusk species associated with red mangroves (*Rhizophora mangle*). Insect and avifauna from the nearby Talara Tar Seeps also suggest warmer, wetter conditions in the Late Pleistocene (70, 71). These mollusks and mangroves require at least seasonal inputs from rainfall and fresh-water streams. Amotape deposits at Sitio Siches itself also contain these mollusks, suggesting that warmer, wetter Late Pleistocene conditions persisted into the Early Holocene (62). Mollusks in Siches-phase deposits are exclusively warm-water animals, but deposits from the subsequent Honda phase have a mix of warm- and cool-water mollusks typical of the area today (62). Mangroves are not present in the area now and local streams are intermittent.

Fish recovered from the site also show a temporal trend (65). Like the mollusks, fish suggest warm-water conditions prevailed during the Amotape phase. During the Siches phase, coastal waters were even warmer, consistent with isotopic values in sea catfish otoliths (*Galeichthys peruvianus*; ref. 63; discussed below). Variations in fishing strategies across the Siches phase may reflect sharper annual or seasonal fluctuations in SST than during the Amotape or Honda occupations. The Honda collection reflects modern conditions at the frontier between the Panamanian and Peru–Chilean provinces.

Coastal assemblages from similar latitudes are broadly comparable between ~12.7 and 4.0 ka (8, 63, 65, 72, 73). South of 12°S, indicator groups are dominated by cool-water animals regardless of time period. Between 10°S and 8°S, warm-water animals decline over time as cool-water species increase, with a major transition at ~5.8 ka. Use of warm-water animals declines slightly *ca*. 5.8 ka at Sitio Siches, just south of 4°S, although these taxa continue to be abundant compared to assemblages further south. Between 4°S and 2°S an early emphasis on warm-water animals persisted and may have intensified over time. Commonalities among assemblages within similar latitudes suggest these patterns reflect larger environmental factors influencing regional economies rather than cultural dynamics alone. The predominance of warm-water species at pre-5.8-ka sites north of 8°S argues against the interpretation that warm-water organisms in northern sites are the result of migrant animals responding to unique geographic situations producing very localized warm conditions (e.g., ref. 19, p. 289).

The biogeographic approach must be used cautiously. It assumes that critical behaviors, such as feeding, reproduction, and habitat preferences, have changed little over the last few millennia. For populations at the extreme ends of a species' preferred habitat, this assumption may be unfounded. The approach also presumes that changes in environmental variables, such as temperature or humidity, are associated with observable changes in archaeological materials. It must take human decision-making into account. Choices about what to use, when to use it, how to use it, how to discard it, and other issues are conditioned by a wide range of cultural criteria beyond simple availability or foraging efficiency. This "cultural imprinting" or "cultural filter" is fundamental to all zooarchaeological interpretations (ref. 74, p. 471; ref. 75, pp. 5–7; and ref. 76, p. 5).

These problems notwithstanding, a multiproxy assessment of indicator groups on regional and temporal scales allows archaeologists to offer insights into former environmental conditions along the Peruvian coast and to evaluate the role of EN in both environmental and cultural change.

Geochemical Analyses. Analysis of $\delta^{18}O$ from $CaCO_3$ biominerals, such as foraminifera and corals, is a powerful and widely used tool for reconstructing past water temperatures. This approach is limited in coastal Peru by a scarcity of appropriate samples. Corals are absent and high temporal resolution in natural death assemblages is rare in the Holocene though useful when found. Mollusk valves and fish otoliths from coastal sites provide the most abundant, temporally well-resolved Holocene $CaCO_3$ remains. These can be valuable for sclerochronological reconstructions of past water temperature, sometimes at a seasonal time scale (77), but the taxa from these sites are often less than ideal for assessing past EN conditions. They are short-lived, preventing direct measurement of EN frequency, and some favor climate regimes and habitats that may bias their interpretation toward cool (e.g., *Mesodesma donacium* [surf clam]) or warm (e.g., *Trachycardium procerum* [cockle]) periods. In addition, all oxygen isotope records are subject to uncertainties about past fluctuations in water $\delta^{18}O$ values, which limit the precision and accuracy of paleotemperature reconstructions even in arid regions like Peru where continental runoff is minimal.

Published records are therefore sometimes contradictory and no reconstruction can be viewed as conclusive. One point on which nearly all sources agree, or at least do not contradict, however, is that EN frequency was low until late in the Middle Holocene and generally increased thereafter (e.g., refs. 61, 63, 78, and 79). The mean state of Holocene water temperatures is less certain. Most SST reconstructions utilize *Mesodesma*, but this species was absent from the north coast for much of the Holocene because it does not tolerate warm SSTs. Consequently, most of these studies do not cover the region of the Peruvian coast most strongly impacted by EN and therefore tend to indicate cooler conditions than may actually have prevailed on the north coast in the early Middle Holocene (e.g., refs. 61 and 78–80). Studies that analyze $\delta^{18}O$ values in taxa that do tolerate warm water, such as sea catfishes and cockles, find evidence for seasonally warmer conditions in the early Middle Holocene at 9°S and permanently warmer conditions at 4°25′S (63, 81, 82). The strength of these conclusions, though, is limited by low-resolution sampling, small sample sizes, and questions related to the habitats and mobility of these species (e.g., ref. 82). In contrast, otolith data from Dufour et al. (83), although based on a single otolith, suggest Middle Holocene water temperatures similar to, or slightly cooler than, today in the Chicama Valley (~8°S).

The mean SST gradient can be reconstructed by comparing paleotemperature data from Peru to reconstructions across the Pacific (e.g., ref. 61), though different manifestations of EN events (e.g., COA and CP) (discussed above) complicate these efforts. CP warms the Central Pacific but has little to no effect on Peru coast SST, while COA causes intense warming on the Peru coast north

Downloaded by guest on April 13, 2020

of 12°S but has little effect in the central Pacific (discussed above), making it difficult to link the local coastal climate experienced by people in Peru in the past to overall Pacific basin conditions.

Another approach to understanding Holocene EN conditions on the Peruvian coast measures radiocarbon in marine shells of independently known age to reconstruct past radiocarbon reservoir effects caused by upwelling fluctuations related to EN (e.g., refs. 84 and 85). As with $\delta^{18}O$ records, reservoir data from short-lived taxa prevent direct assessment of EN frequency but may yield insight into mean state. Again, most reservoir effect data are from too far south of the direct EN impact zone (e.g., refs. 86–88) to give confident insight into EN history and its effect on much of Peru, but these records do confirm a variable reservoir effect over the Holocene. Records from locations farther north, where the impact of EN was more direct, are few and restricted to the later Holocene, but they tend to confirm the interpretation of other proxy data that sustained and prolonged EN conditions occurred in the centuries prior to ~800 AD (~1.15 ka) (89).

Isotopic records of past coastal Peruvian climate continue to be refined with additional validation studies (e.g., refs. 90–94) and ongoing applications to ancient samples (e.g., ref. 95). The strength of these proxies is their record of local conditions experienced by a site's inhabitants rather than relying on inferences of local conditions derived from distant proxies. Their utility, however, is limited by factors outlined above, which contribute to sometimes contradictory reconstructions.

Discussion: Holocene EN in Peru from Archaeological Proxies

Beginning in the 1980s, we and our colleagues began reconstructing Holocene EP frequency using biogeographic and geochemical analyses of archaeological mollusks and fish (Fig. 2*A*) (6–10, 62, 63, 65, 96). We proposed that EP (the only flavor then known) was present prior to 8.0 to 9.0 ka but of unknown frequency and then during the early Middle Holocene (~8.0 to 5.8 ka) was absent or much less frequent. During the early Middle Holocene, average SST along the north coast was warmer than present, with enhanced seasonal amplitude at 9°S and a similar-to-modern seasonal amplitude with warmer SST throughout the year at 4°25′S. This situation differs from modern manifestations of EN. From 5.8 to 2.9 ka, EP was present but less frequent than later, occurring perhaps once or twice per century. At about 2.9 ka, EP became much more frequent and then fluctuated around its modern periodicity. In light of the 2017 COA, we now suspect that our north coast record may include both COA and EP events, which are indistinguishable in our data. Other natural proxy records seemed to confirm the broad outline of our Holocene EN reconstruction, in some cases quite closely (e.g., refs. 48, 49, 54, 97, and 98).

Some researchers report different results. Carré et al. (ref. 61, p. 1045) found (Fig. 2*B*) that "ENSO variance was close to the modern level in the early Holocene and severely damped ~4–5 ka. In addition, ENSO variability was skewed toward cold events along coastal Peru 6.7–7.5 ka owing to a shift of warm anomalies toward the Central Pacific. The modern ENSO regime was established ~3–4.5 ka." They base this reconstruction of EN frequencies on geochemical analyses of *Mesodesma* from coastal Peruvian archaeological sites at and south of ~12°S. Their interpretation of Early and Late Holocene EN frequency for the central and southern coast is essentially the same as our reconstruction for north of 12°S, although we hypothesize a more abrupt transition just after 3.0 ka. For the early Middle Holocene, Carré et al. (61) propose cool events related to CP-like warming in the central Pacific, whereas our north coast record indicates warming. We agree on a dampened ENSO signal in the late Middle Holocene but suggest that dampening started earlier and lasted longer on the north coast.

One indicator of different Holocene climate regimes on the north and south coasts is that *Mesodesma* surf clams are present on the north coast only between about 5.8 and 2.9 ka even though they are common in middens of all periods south of 12°S (9, 62). Peruvian *Mesodesma* do not tolerate warming associated with either EP or COA, and the patterning of their presence suggests a pre-5.8-ka warming, low-frequency EP (which might have included COA) between 5.8 and 2.9 ka, and thereafter a higher frequency EP (+COA) on the north coast.

Both archaeological proxy-based EN reconstructions may be correct, reflecting the presence of a long-term climate divide at ~12°S. The SST pattern of COA is consistent with multiple lines of evidence (16–20) for this divide. Hu et al. (32) identified 7 COA events between 1979 and 2017. Three were associated with large-magnitude EP events; EP and COA events would not be distinguishable in the paleorecord. We examined pentadal SST data for the other 4 early-21st-century COA events (2008, 2014, 2015, and 2017) at Chimbote, Callao, Pisco, and Ilo (*SI Appendix*, Figs. S1–S3) and found a much stronger SST signal at and north of 12°S than south of that point.

Much of the world was warmer during the early Middle Holocene (e.g., ref. 99) when our data suggest that the northern Peruvian coast was warmer than the southern Peruvian coast and elsewhere in the tropical Pacific (62). Peng et al.'s (100) climate model projects an increase in extreme COAs like the 2017 event under global warming. We suggest that early Middle Holocene global warming caused frequent COA events and a warmer north coast.

Given that COA events raise SST on the Peruvian north coast but not in the central Pacific, and that CP events raise SST in the Central Pacific but not on the Peruvian coast, it is unclear what central Pacific paleoclimate records (e.g., refs. 101 and 102) will tell us about EN behavior on the Peruvian coast until the chronology for these flavors is better known.

Conclusion

Archaeological sites are indeed "distributed observing networks of the past." They record conditions from every ecosystem and time period important to human history and provide proxies where more traditional ones are absent, rare, or compromised. In addition to Peru, other Pacific Basin studies have used archaeological deposits to track past EN behavior (e.g., Australia: refs. 103–105; California: refs. 106 and 107; Chile: ref. 105; central Pacific: ref. 108), and additional archaeological proxies should be developed. For the Peruvian coast, we conclude that archaeological climate records are among the most direct and useful for understanding the full complexity of Holocene EN.

Chief among the challenges ahead are finding ways to recognize the individual flavors of EN through new analytic techniques, determining the time depth of these flavors, and assessing the hypothesis that COA was the normal state on the north coast of Peru during the early Middle Holocene. The results are crucial for unraveling the full story of EN through time, contributing to modeling exercises to predict future EN behavior, and understanding human ecodynamics that impact lives and livelihoods.

Data Availability. This paper contains no new data.

Downloaded by guest on April 13, 2020

1 E. Shropshire, *Blame it on El Niño. Released on the Album Love, Death, and Taxes by Dr. Elmo* (Laughing Stock, 2000).
2 W. Cai *et al.*, Increased frequency of extreme La Niña events under greenhouse warming. *Nat. Clim. Chang.* **5**, 849–859 (2015).
3 Z. Lu, Z. Liu, J. Zhu, K. M. Cobb, A review of paleo El Niño-Southern Oscillation. *Atmosphere* **9**, 130 (2018).
4 D. H. Sandweiss, A. R. Kelley, Archaeological contributions to climate change research: The archaeological record as a paleoclimatic and paleoenvironmental archive. *Annu. Rev. Anthropol.* **41**, 371–391 (2012).
5 G. Hambrecht *et al.*, Archaeological sites as distributed long-term observing networks of the past (DONOP). *Quat. Int.*, 10.1016/j.quaint.2018.04.016 (2018).
6 D. H. Sandweiss *et al.*, "Mid-Holocene climate and culture change in coastal Peru" in *Climatic Change and Cultural Dynamics: A Global Perspective on Mid-Holocene Transitions*, D. G. Anderson, K. A. Maasch, D. H. Sandweiss, Eds. (Academic, 2007), pp. 25–50.
7 H. B. Rollins, J. B. Richardson, III, D. H. Sandweiss, The birth of El Niño: Geoarchaeological evidence and implications. *Geoarchaeology* **1**, 3–15 (1986).
8 D. H. Sandweiss, J. B. Richardson, III, E. J. Reitz, H. B. Rollins, K. A. Maasch, Geoarchaeological evidence from Peru for a 5000 Years B.P. onset of El Niño. *Science* **273**, 1531–1533 (1996).
9 D. H. Sandweiss *et al.*, Variation in Holocene El Niño frequencies: Climate records and cultural consequences in ancient Peru. *Geology* **29**, 603–606 (2001).
10 D. H. Sandweiss, K. A. Maasch, F. Chai, C. F. T. Andrus, E. J. Reitz, Geoarchaeological evidence for multi-decadal natural climatic variability and ancient Peruvian fisheries. *Quat. Res.* **61**, 330–334 (2004).
11 G. T. Rustic, A. Koutavas, T. M. Marchitto, B. K. Linsley, Dynamical excitation of the tropical Pacific Ocean and ENSO variability by Little Ice Age cooling. *Science* **350**, 1537–1541 (2015).
12 B. Fitzhugh, V. L. Butler, K. M. Bovy, M. A. Etnier, Human ecodynamics: A perspective for the study of long-term change in socioecological systems. *J. Archaeol. Sci. Rep.* **23**, 1077–1094 (2019).
13 B. Orlove, Human adaptation to climate change: A review of three historical cases and some general perspectives. *Environ. Sci. Policy* **8**, 589–600 (2005).
14 K. W. Butzer, Collapse, environment, and society. *Proc. Natl. Acad. Sci. U.S.A.* **109**, 3632–3639 (2012).
15 G. M. Feinman, D. M. Carballo, Collaborative and competitive strategies in the variability and resiliency of large-scale societies in Mesoamerica. *Econ. Anthropol.* **5**, 7–19 (2018).
16 T. J. DeVries, H. Schrader, Variation of upwelling/oceanic conditions during the latest Pleistocene through Holocene on the central Peruvian coast: A diatom record. *Mar. Micropaleontol.* **6**, 157–167 (1981).
17 P. W. Rundel *et al.*, The phytogeography and ecology of the coastal Atacama and Peruvian Deserts. *Aliso* **13**, 1–49 (1991).
18 P. W. Rundel, M. O. Dillon, Ecological patterns in the Bromeliaceae of the lomas formations of coastal Chile and Peru. *Plant Syst. Evol.* **212**, 261–278 (1998).
19 R. Salvatteci, R. R. Schneider, T. Blanz, E. Mollier-Vogel, Deglacial to Holocene ocean temperatures in the Humboldt Current System as indicated by alkenone paleothermometry. *Geophys. Res. Lett.* **46**, 281–292 (2019).
20 J. S. Noller, "Late cenozoic stratigraphy and soil geomorphology of the Peruvian desert, 3°-18° S: A long-term record of hyperaridity and El Niño," PhD thesis, University of Colorado at Boulder, Boulder, CO (1993).
21 W. Arntz, A. Landa, A. Tarazona, Eds., El fenómeno 'El Niño' y su impacto en la fauna marina. *Bol. Inst. Mar Perú-Callao*, Special Issue, 41–49 (1985).
22 UCAR/NOAA, "El Niño and climate prediction" (Reports to the Nation on Our Changing Planet No. 3, University Corporation for Atmospheric Research, 1994).
23 J. Marcus, K. V. Flannery, J. Sommer, R. G. Reynolds, "Maritime adaptations at Cerro Azul, Peru: A comparison of Late Intermediate and twentieth-century fishing" in *Maritime Communities of the Ancient Andes*, G. Prieto, D. H. Sandweiss, Eds. (University Press of Florida, 2020), pp. 351–365.
24 M. E. Moseley, D. Wagner, J. B. Richardson, III, "Space Shuttle imagery of recent catastrophic change along the arid Andean coast" in *Paleoshorelines and Prehistory: An Investigation of Method*, L. L. Johnson, M. Stright, Eds. (CRC Press, 1992), pp. 215–235.
25 D. H. Sandweiss, The beach ridges at Santa, Peru: El Niño, uplift, and prehistory. *Geoarchaeology* **1**, 17–28 (1986).
26 S. Shafer Rogers, D. H. Sandweiss, K. A. Maasch, D. F. Belknap, P. Agouris, Coastal change and beach ridges along the northwest coast of Peru: Image and GIS analysis of the Chira, Piura, and Colán beach-ridge plains. *J. Coast. Res.* **20**, 1102–1125 (2004).
27 L. E. Wells, L.E. Holocene landscape change on the Santa Delta, Peru: Impact on archaeological site distributions. *Holocene* **2**, 193–204 (1992).
28 J. B. Richardson, III, The Chira Beach Ridges, sea level change, and the origins of maritime economies on the Peruvian coast. *Ann. Carnegie Mus.* **52**, 265–276 (1983).
29 D. F. Belknap, D. H. D. H. Sandweiss, Effect of the Spanish Conquest on coastal change in Northwestern Peru. *Proc. Natl. Acad. Sci. U.S.A.* **111**, 7986–7989 (2014).
30 A. S. Gagnon, K. E. Smoyer-Tomic, A. B. Bush, The El Niño southern oscillation and malaria epidemics in South America. *Int. J. Biometeorol.* **46**, 81–89 (2002).
31 R. S. Kovats, M. J. Bouma, S. Hajat, E. Worrall, A. Haines, El Niño and health. *Lancet* **362**, 1481–1489 (2003).
32 Z.-Z. Hu, B. Huang, J. Zhu, A. Kumar, M. J. McPhaden, On the variety of coastal El Niño events. *Clim. Dyn.* **52**, 7537–7552 (2019).
33 K. Takahashi, A. G. Martínez, The very strong coastal El Niño in 1925 in the far-eastern Pacific. *Clim. Dyn.* **52**, 7389–7415 (2019).
34 A. Caramanica, Resilience and resistance in the Peruvian Deserts. *ReVista Harv. Rev. Lat. Am.* **13**, 48–50 (2018).
35 RPP (Radio Prográmas del Perú), Las cifras que van dejando las lluvias en Perú (2017). https://rpp.pe/peru/actualidad/mas-de-56-mil-damnificados-por-la-temporada-de-lluvias-a-nivel-nacional-noticia-1036219 . Accessed 7 November 2019.
36 K. Ashok, S. K. Behera, S. A. Rao, H. Weng, T. Yamagata, El Niño Modoki and its possible teleconnection. *J. Geophys. Res.* **112**, C11007 (2007).
37 C. Wang, X. Wang, Classifying El Niño Modoki I and II by different impacts on rainfall in southern China and typhoon tracks. *J. Clim.* **26**, 1322–1338 (2013).
38 A. Taschetto, M. England, El Niño Modoki impacts on Australian rainfall. *J. Clim.* **22**, 3167–3174 (2009).
39 H. Weng, K. Ashok, S. K. Behera, S. A. Rao, T. Yamagata, Anomalous winter climate conditions in the Pacific rim during recent El Niño Modoki and El Niño events. *Clim. Dyn.* **32**, 663–674 (2009).
40 W. Zhang, F.-F. Jin, A. Turner, Increasing autumn drought over southern China associated with ENSO regime shift. *Geophys. Res. Lett.* **41**, 4030–4026 (2014).
41 P. Rau *et al.*, Regionalization of rainfall over the Peruvian Pacific slope and coast. *Int. J. Climatol.* **37**, 143–158 (2017).
42 J. Sulca, K. Takahashi, J.-C. Espinoza, M. Vuille, W. Lavado-Casimiro, Impacts of different ENSO flavors and tropical Pacific convection variability (ITCZ, SPCZ) on austral summer rainfall in South America, with a focus on Peru. *Int. J. Climatol.* **38**, 420–435 (2018).
43 M. H. Glantz, Ed., *La Niña and Its Impacts: Facts and Speculation* (United Nations University Press, 2002).
44 M. J. McPhaden, "El Niño and La Niña: Causes and global consequences" in *Encyclopedia of Global Environmental Change. The Earth System: Physical and Chemical Dimensions of Global Environmental Change*, M. C. MacCracken, J. S. Perry, Eds. (Wiley, 2003), pp. 353–370, **vol. 1**.
45 N. Ordinola, "The consequences of cold events for Peru" in *La Niña and its Impacts: Facts and Speculation*, M. H. Glantz, Ed. (United Nations University Press, 2002), pp. 146–150.
46 C. R. Chazen, M. A. Altabet, D. T. Herbert, Abrupt mid-Holocene onset of centennial-scale climate variability on the Peru-Chile Margin. *Geophys. Res. Lett.* **36**, L18704 (2009).
47 T. J. DeVries, W. G. Pearcy, Fish sediments in debris of the upwelling zone off central Peru: A late Quaternary record. *Deep Sea Res. A Oceanogr. Res. Pap.* **28**, 87–109 (1982).
48 B. Rein *et al.*, El Niño variability off Peru during the last 20,000 years. *Paleoceanography* **20**, PA4003 (2005).
49 C. G. Skilbeck, D. Fink, Data report: Radiocarbon dating and sedimentation rates for Holocene–Upper Pleistocene sediments, eastern equatorial Pacific and Peru continental margin. *Proc. Ocean Drill. Program Sci. Results* **201**, 1–15 (2006).
50 M. C. Makou, T. I. Eglinton, D. W. Oppo, K. A. Hughen, Postglacial changes in El Niño and La Niña behavior. *Geology* **38**, 43–46 (2010).

Downloaded by guest on April 13, 2020

51 B. R. Billman, G. Huckleberry, "Deciphering the politics of prehistoric El Niño events on the north coast of Peru" in *El Niño, Catastrophism, and Culture Change in Ancient America*, D. H. Sandweiss, J. Quilter, Ed. (Dumbarton Oaks Research Library & Collection/Harvard University Press, 2008), pp. 101–113.
52 L. E. Wells, Holocene history of the El Niño phenomenon as recorded in flood sediments of northern coastal Peru. *Geology* **18**, 1134–1137 (1990).
53 G. Huckleberry, F. Hayashida, J. Johnson, New insights into the evolution of an intervalley prehistoric irrigation canal system, North Coastal Peru. *Geoarchaeology* **27**, 492–520 (2012).
54 D. T. Rodbell *et al.*, An approximately 15,000-year record of El Niño-driven alluviation in southwestern Ecuador. *Science* **283**, 516–520 (1999).
55 C. M. Moy, G. O. Seltzer, D. T. Rodbell, D. M. Anderson, Variability of El Niño/Southern Oscillation activity at millennial timescales during the Holocene epoch. *Nature* **420**, 162–165 (2002).
56 T. Schneider, H. Hampel, P. V. Mosquera, W. Tylmann, M. Grosjean, Paleo-ENSO revisited: Ecuadorian Lake Pallcacocha does not reveal a conclusive El Niño signal. *Global Planet. Change* **168**, 54–66 (2018).
57 L. G. Thompson, E. Mosley-Thompson, J. F. Bolzan, B. R. Koci, A 1500-year record of tropical precipitation in ice cores from the Quelccaya Ice Cap, Peru. *Science* **229**, 971–973 (1985).
58 L. G. Thompson *et al.*, Annually resolved ice core records of tropical climate variability over the past ~1800 years. *Science* **340**, 945–950 (2013).
59 J. Kiefer, C. Karamperidou, High-resolution modeling of ENSO-induced precipitation in the tropical Andes: Implications for proxy interpretation. *Paleoceanogr. Paleoclimatol.* **34**, 217–236 (2019).
60 J. V. Hurley, M. Vuille, D. R. Hardy, On the interpretation of the ENSO signal embedded in the stable isotopic composition of Quelccaya Ice Cap, Peru. *J. Geophys. Res. Atmos.* **124**, 131–145 (2019).
61 M. Carré *et al.*, Holocene history of ENSO variance and asymmetry in the eastern tropical Pacific. *Science* **345**, 1045–1048 (2014).
62 D. H. Sandweiss, Terminal Pleistocene through Mid-Holocene archaeological sites as paleoclimatic archives for the Peruvian coast. *Palaeogeogr. Palaeoclimatol. Palaeoecol.* **194**, 23–40 (2003).
63 C. F. T. Andrus, D. E. Crowe, D. H. Sandweiss, E. J. Reitz, C. S. Romanek, Otolith δ^{18}O record of mid-Holocene sea surface temperatures in Peru. *Science* **295**, 1508–1511 (2002).
64 H. K. Kenward, A. Hall, Enhancing bioarchaeological interpretation using indicator groups: Stable manure as a paradigm. *J. Archaeol. Sci.* **24**, 663–673 (1997).
65 E. J. Reitz, D. H. Sandweiss, N. R. Cannarozzi, Fishing on the frontier: Vertebrate remains from Amotape, Siches, and Honda Phase occupations at Sitio Siches (PV 7-19), Peru. *Fla. Mus. Natural Hist. Bull.* **56**, 109–181 (2019).
66 F. L. Scartascini, The role of ancient fishing on the desert coast of Patagonia, Argentina. *J. Island Coast. Archaeol.* **12**, 115–132 (2017).
67 N. F. Chirichigno, *Catálogo de especies marinas de interés económico actual o potencial para América Latina: Parte II, Pacífico Centro y Suroriental* (FAO, 1982).
68 J. B. Richardson, III, "The Preceramic sequence and the Pleistocene and Post-Pleistocene climate of northwest Peru" in *Variations in Anthropology: Essays in Honor of John C. McGregor*, D. Lathrap, J. Douglas, Eds. (Illinois Archaeological Survey, 1973), pp. 199–211.
69 J. B. Richardson, III, "Early man on the Peruvian north coast, early maritime exploitation and Pleistocene and Holocene environment" in *Early Man in America from a Circum-Pacific Perspective*, A. L. Bryan, Ed. (Occasional Paper No. 1, Department of Anthropology, University of Alberta, 1978), pp. 274–289.
70 K. E. Campbell, "Late Pleistocene events along the coastal plain of Northwestern Peru" in *Biological Diversity in the Tropics*, G. Prance, Ed. (Columbia University Press, 1982), pp. 423–440.
71 C. S. Churcher, The insect fauna from the Talara Tar Seeps, Peru. *Can. J. Zool.* **44**, 935–993 (1966).
72 E. J. Reitz, Fishing in Peru between 10000 and 3750 BP. *Int. J. Osteoarchaeol.* **11**, 163–171 (2001).
73 E. J. Reitz, S. D. DeFrance, D. H. Sandweiss, H. E. McInnis, Flexibility in southern Peru coastal economies: A vertebrate perspective on the Terminal Pleistocene/Holocene transition. *J. Island Coast. Archaeol.* **10**, 155–183 (2015).
74 H. B. Rollins, D. H. Sandweiss, J. C. Rollins, "Mollusks and coastal archaeology; A review" in *Decade of North American Geology, Centennial Special Volume 4: Archaeological Geology of North America*, N. P. Lasca, J. D. Donahue, Eds. (Geological Society of America, 1990), pp. 467–478.
75 E. J. Reitz, E. S. Wing, *Zooarchaeology* (Cambridge University Press, ed. 2, 2008).
76 E. J. Reitz, M. Shackley, *Environmental Archaeology* (Springer, 2012).
77 C. F. T. Andrus, Shell midden sclerochronology. *Quat. Sci. Rev.* **30**, 2892–2905 (2011).
78 M. Carré *et al.*, Mid-Holocene mean climate in the south-eastern Pacific and its influence on South America. *Quat. Int.* **253**, 55–66 (2012).
79 P. Loubere, W. Creamer, J. Haas, Evolution of the El Nino-Southern Oscillation in the late Holocene and insolation driven change in the tropical annual SST cycle. *Global Planet. Change* **100**, 129–144 (2013).
80 M. Carré, I. Bentaleb, M. Fontugne, D. Lavallée, Strong El Niño events during the early Holocene: Stable isotope evidence from Peruvian sea-shells. *Holocene* **15**, 42–47 (2005).
81 C. F. T. Andrus, D. H. Sandweiss, E. J. Reitz, "Climate change and archaeology: The Holocene history of El Niño on the coast of Peru" in *Case Studies in Environmental Archaeology*, E. J. Reitz, M. C. Scarry, S. J. Scudder, Eds. (Plenum, ed. 2, 2008), pp. 143–157.
82 C. F. T. Andrus *et al.*, Response to comment on "Otolith δ ^{18}O record of Mid-Holocene sea surface temperatures in Peru". *Science* **299**, 203b (2003).
83 E. Dufour, O. Trombret, P. Béarez, "Fish otoliths from Huaca Prieta" in *Where the Land Meets the Sea: Fourteen Millennia of Human Prehistory on the North Coast of Peru*, T. D. Dillehay, Ed. (University of Texas Press, 2017), pp. 705–711.
84 C. F. T. Andrus, G. W. L. Hodgins, D. H. Sandweiss, D. E. Crowe, "Molluscan radiocarbon as a proxy for El Niño-related upwelling variation in Peru" in *Isotopic and Elemental Tracers of Late Quaternary Climate Change*, D. Surge, G. Mora, Eds. (Geological Society Special Publications, 2005), **vol. 395**, pp. 13–19.
85 K. B. Jones, G. W. L. Hodgins, M. F. Etayo-Cadavid, C. F. T. Andrus, D. H. Sandweiss, Centuries of marine radiocarbon reservoir age variation within archaeological *Mesodesma donacium* shells from southern Peru. *Radiocarbon* **52**, 1207–1214 (2010).
86 M. Fontugne, P. Usselmann, D. Lavallée, M. Julien, C. Hatté, El Niño variability in the coastal desert of southern Peru during the Mid-Holocene. *Quat. Res.* **52**, 171–179 (1999).
87 L. Ortlieb, G. Vargas, J. F. Saliège, Marine radiocarbon reservoir effect along the northern Chile-southern Peru coast (14–24°S) throughout the Holocene. *Quat. Res.* **75**, 91–103 (2010).
88 K. B. Jones, G. W. L. Hodgins, C. F. T. Andrus, M. F. Etayo-Cadavid, Modeling molluscan marine reservoir ages in a variable-upwelling environment. *Palaios* **25**, 126–131 (2010).
89 M. F. Etayo-Cadavid *et al.*, Marine radiocarbon reservoir age variation in *Donax obesulus* shells from Northern Peru: Late Holocene evidence for extended El Niño. *Geology* **41**, 599–602 (2013).
90 C. E. Lazareth, C. Liétard, C. Pierre, L. Ortlieb, Inter-individual and inter-site reproducibility of δ^{18}O profiles across *Protothaca thaca* (Bivalvia, Veneridae) shells from Peru and Chile. *Geophys. Res. Abstr.* **10**, EGU2008–A-06203 (2008).
91 K. B. Jones, G. W. L. Hodgins, M. F. Etayo-Cadavid, C. F. T. Andrus, Upwelling signals in radiocarbon from early 20th-century Peruvian bay scallop (*Argopecten purpuratus*) shells. *Quat. Res.* **72**, 452–456 (2009).
92 J. Sadler *et al.*, Reconstructing past upwelling intensity and the seasonal dynamics of primary productivity along the Peruvian coastline from mollusk shell stable isotopes. *Geochem. Geophys. Geosyst.* **13**, Q01015 (2012).
93 J. Wei, C. F. T. Andrus, A. Perez-Huerta, "*Semele corrugata* microstructure and oxygen isotope profiles as indicators of seasonality" in *Where the Land Meets the Sea: Fourteen Millennia of Human Prehistory on the North Coast of Peru*, T. D. Dillehay, Ed. (University of Texas Press, 2017), pp. 714–722.
94 M. F. Etayo-Cadavid, C. F. T. Andrus, K. B. Jones, G. W. L. Hodgins, Subseasonal variations in marine radiocarbon reservoir age from pre-bomb *Donax obesulus* and *Protothaca asperrima* shell carbonate. *Chem. Geol.* **526**, 110–116 (2018).

Downloaded by guest on April 13, 2020

95 J. Warner *et al*., Local perspectives on ENSO variability 2300 BP and now: Evidence from two short lived intertidal bivalves: *Mesodesma donacium* and *Donax obesulus* (abstract PP43D-1958). *American Geophysical Union Fall Meeting 2018* (American Geophysical Union, 2018).
96 E. J. Reitz, D. H. Sandweiss, Environmental change at Ostra Base Camp, A Peruvian preceramic site. *J. Archaeol. Sci.* **28**, 1085–1100 (2001).
97 B. Jenny *et al*., Early to Mid-Holocene aridity in central Chile and the southern Westerlies: The Laguna Aculeo record (341S). *Quat. Res.* **58**, 160–170 (2002).
98 M. A. Riedinger, M. Steinitz-Kannan, W. M. Last, M. Brenner, A ~6100 ^{14}C yr record of El Niño activity from the Galapagos Islands. *J. Paleolimnol.* **27**, 1–7 (2002).
99 P. A. Mayewski *et al*., Holocene climate variability. *Quat. Res.* **62**, 243–255 (2004).
100 Q. Peng, S.-P. Xie, D. Wang, X.-T. Zheng, H. Zhang, Coupled ocean-atmosphere dynamics of the 2017 extreme coastal El Niño. *Nat. Commun.* **10**, 298 (2019).
101 K. M. Cobb *et al*., Highly variable El Niño-Southern Oscillation throughout the Holocene. *Science* **339**, 67–70 (2013).
102 C. Karamperidou, P. N. Di Nezio, A. Timmermann, F.-F. Jin, K. M. Cobb, The response of ENSO flavors to mid-Holocene climate: Implications for proxy interpretation. *Paleoceanography* **30**, 527–547 (2015).
103 B. Asmussen, P. McInnes, Assessing the impact of mid-to-late Holocene ENSO-driven climate change on toxic *Macrozamia* seed use: A 5000 year record from eastern Australia. *J. Archaeol. Sci.* **40**, 471–480 (2013).
104 P. Veth, P. Hiscock, A. Williams, Are tulas and ENSO linked in Australia? *Aust. Archaeol.* **72**, 7–14 (2011).
105 A. Williams, C. M. Santoro, M. A. Smith, C. Latorre, The impact of ENSO in the Atacama Desert and Australian arid zone: Exploratory time-series. *Chungara (Arica)* **40E**, 245–259 (2008).
106 D. J. Kennett, J. P. Kennett, J. M. Erlandson, K. G. Canariato, Human response to middle Holocene climate change on California's Channel Islands. *Quat. Sci. Rev.* **26**, 351–367 (2007).
107 P.M. Masters, Holocene sand beaches of southern California: ENSO forcing and coastal processes on millennial scales. *Palaeogeogr. Palaeoclimatol. Palaeoecol.* **232**, 73–95 (2006).
108 A. B. J. Lambrides, M. I. Weisler, Late Holocene Marshall Islands archaeological tuna records provide proxy evidence for ENSO variability in the Western and Central Pacific Ocean. *J. Island Coast. Archaeol.* **13**, 531–562 (2018).

Downloaded by guest on April 13, 2020